



Supplement of

Observed change and the extent of coherence in the Gulf Stream system

Helene Asbjørnsen et al.

Correspondence to: Helene Asbjørnsen (h.asbjornsen@uib.no)

The copyright of individual parts of the supplement might differ from the article licence.

Contents of this supplementary

Section transports in ECCOv4-r4

Table S1-S2

Figure S1-S9

Section transports in ECCOv4-r4

Florida Current and Western Boundary Current: At 26.58°N , the Florida Current transport is the net volume transport on the continental shelf (76.50°W to 81.50°W) while the Western Boundary Current additionally includes the northward transport in the secondary branch east of the shelf (73.50°W to 76.5°W).

Gulf Stream at Oleander section: Upper-ocean (0-1155 m) northeastward volume transport along the Oleander transect from New Jersey to Bermuda.

NAC at OSNAP-East: Net volume transport east of 25.6°W and above the 27.66 kg/m^3 isopycnal along the OSNAP-East section.

Greenland-Scotland Ridge inflow: The three inflow sections are located similarly to those in observations (see Figure 2). Only volume transport into the Nordic Seas are integrated for the inflow transport (Denmark Strait inflow: only eastward transport, Faroe-Shetland Channel: northeastward transport, Iceland-Faroe Ridge: only eastward transport).

NwASC at Svinøy: Volume transport integral over the Atlantic Water (here $S > 35$ psu) along the Svinøy section from 61.77°N , 5.48°E to 63.84°N , 1.31°E .

NwASC at BSO: Volume transport integral over the Atlantic Water (here $T > 3^{\circ}\text{C}$) at the Barents Sea Opening (BSO; 71.15°N to 73.24°N , 19°E).

Table S 1. Correlation in ECCOv4-r4 when the Ekman layer (0-100m) is removed from the section transports. Correlations (at zero lag time) between the low-pass filtered anomalies from the time mean in ECCOv4-r4 (1992-2017). Significant correlations at the 95% confidence level in bold font (Chelton (1983) method).

	Florida Current	WBC	Oleander GS	OSNAP NAC	GSR	Svinøy	BSO
Florida Current	1	-	-	-	-	-	-
WBC	0.90	1	-	-	-	-	-
Oleander GS	0.69	0.77	1	-	-	-	-
OSNAP NAC	-0.36	-0.32	-0.25	1	-	-	-
GSR	-0.24	-0.44	-0.22	0.16	1	-	-
Svinøy	0.12	-0.01	0.22	0.03	0.65	1	-
BSO	-0.46	-0.65	-0.58	0.31	0.62	0.21	1

Table S 2. Linear trends over components representative of overturning strength. The trends ($[Sv/yr]$) are computed from observational monthly mean transport time series (negative sign denotes weakening). The time periods over which the trends are calculated are given in Table 1. Significant trends at the 95% confidence level in bold font (modified Mann-Kendall trend test for autocorrelated data (Hamed and Rao, 1997)).

Trends in:	Observations
RAPID moc_z	-0.121
OSNAP moc_σ	0.123
GSR overflow	0.015

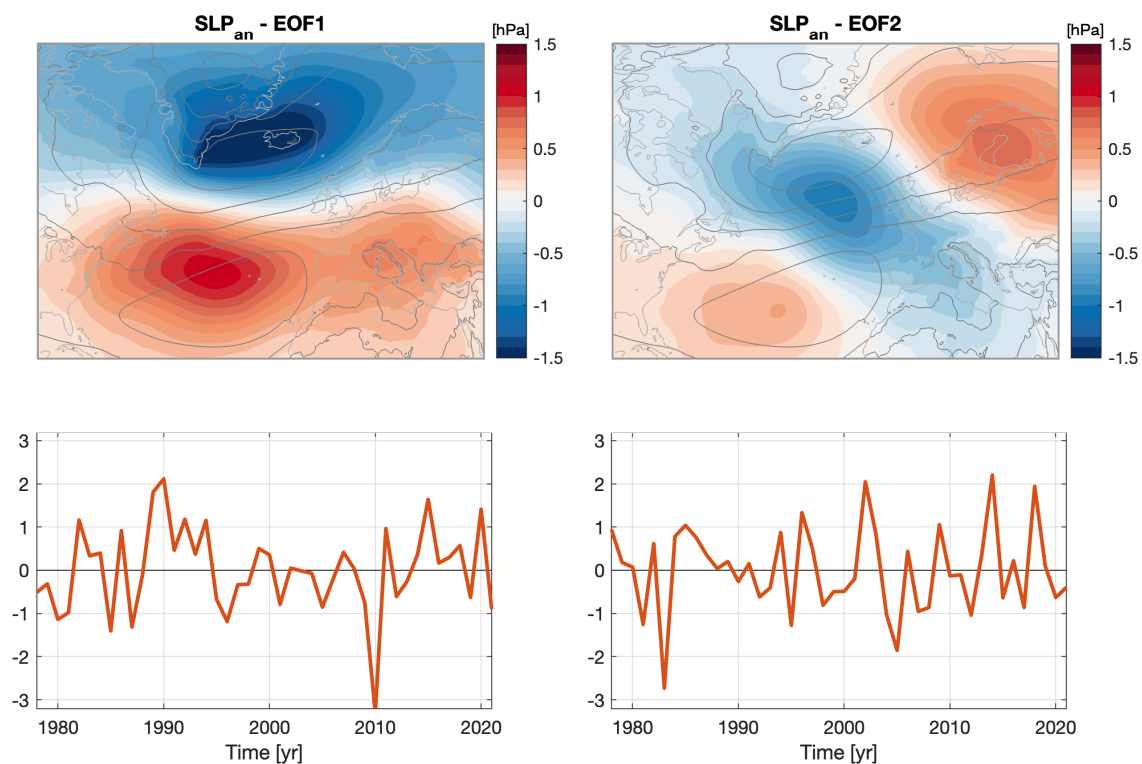


Figure S 1. The leading two EOF modes of North Atlantic (20-80°N, 90°W-40°E) annual mean sea level pressure (SLP) variability from ERA5 in color, and the associated principal component time series. EOF1 (NAO; North Atlantic Oscillation) explains 49% and EOF2 (EAP; East Atlantic Pattern) explains 15% of the variability. Grey contour lines show the climatological annual mean SLP pattern (contours plotted every 3 hPa from 1007 hPa to 1019 hPa). The climatological SLP centre in the north is the Icelandic low and the centre in the south is the Azores high.

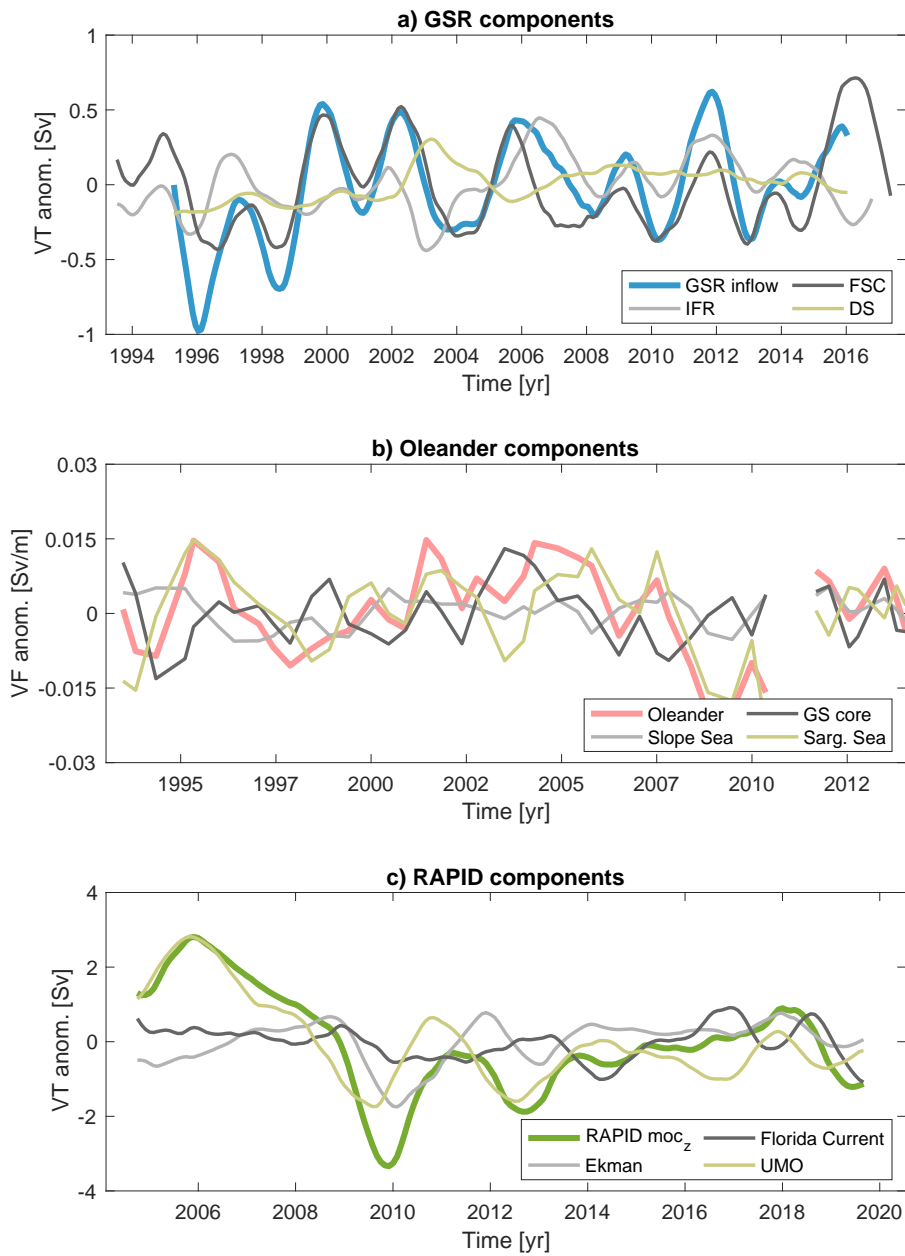


Figure S 2. Decomposition of observational transport records. Transport anomalies from the time-mean at a) the Greenland-Scotland Ridge (IFR; Iceland-Faroe Ridge, FSC; Faroe-Shetland Channel, DS; Denmark Strait), b) the Oleander section (Slope Sea, Gulf Stream core, Sargasso Sea), and c) the RAPID section (Ekman transport, Florida Current, UMO; Upper mid-ocean transport). The Oleander Gulf Stream core is the component used in the main analysis. Note that the Sargasso Sea and Slope Sea components at Oleander, and the UMO component at RAPID have a net southward transport.

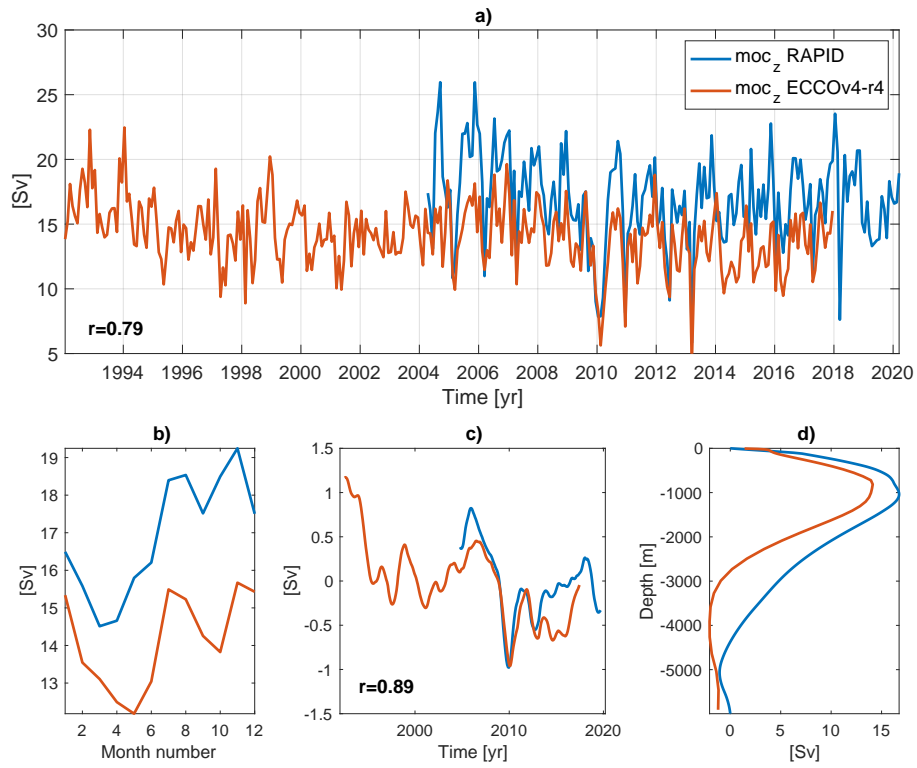


Figure S 3. Comparison between ECCOv4-r4 and observations at RAPID 26.5°N. (a) Monthly mean overturning strength (moc_z), and the (b) seasonal cycle, (c) interannual variability (normalized and 1-year low-pass filtered), (d) and climatological overturning stream function during 2004-2020 for observations and during 1992-2017 for ECCOv4-r4.

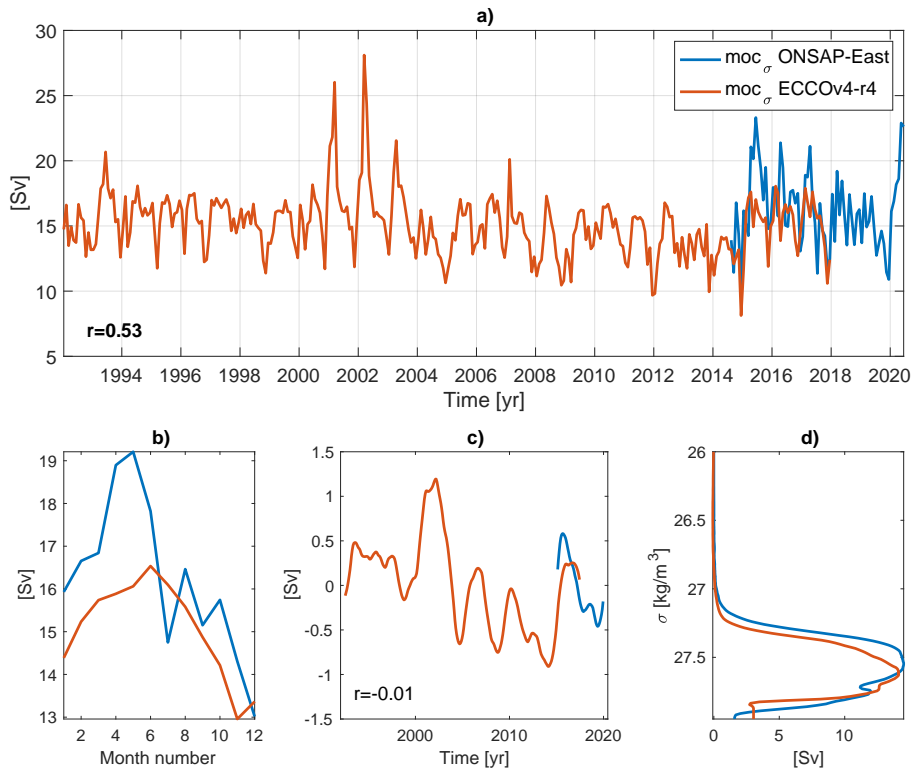


Figure S 4. Comparison between ECCOv4-r4 and observations at OSNAP-East. (a) Monthly mean overturning strength (moc_{σ}), and the (b) seasonal cycle, (c) interannual variability (normalized and 1-year low-pass filtered), and (d) climatological overturning stream function during 2014-2020 for observations and during 1992-2017 for ECCOv4-r4.

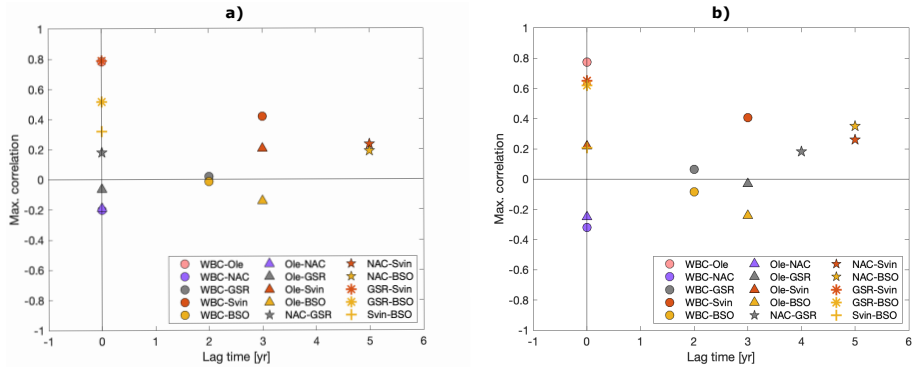


Figure S 5. Maximum correlation between the transport sections in ECCOv4-r4 within 0-6 year lag time. a) As in Table 2, only that maximum correlation with corresponding lag time is displayed. b) As in a), but with the Ekman layer (0-100 m) removed from the section transports. The section name stated second in the legend lags the section name stated first.

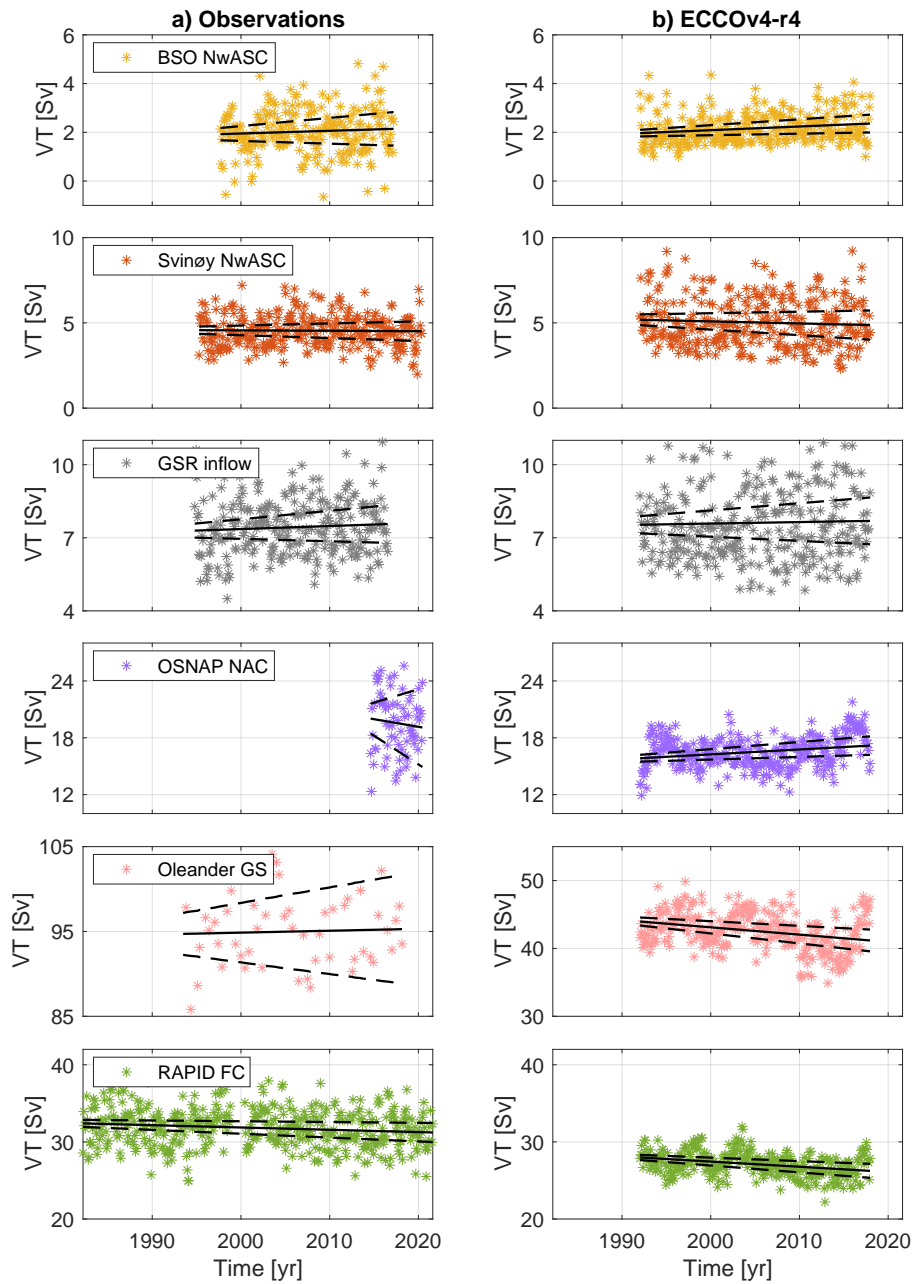


Figure S 6. Confidence interval (95%) for estimated trend in observational and ECCOv4-r4 volume transport time series. Monthly mean transport values are shown in color, with confidence interval marked by dashed black lines. Trend values and significance is given in Table 3.

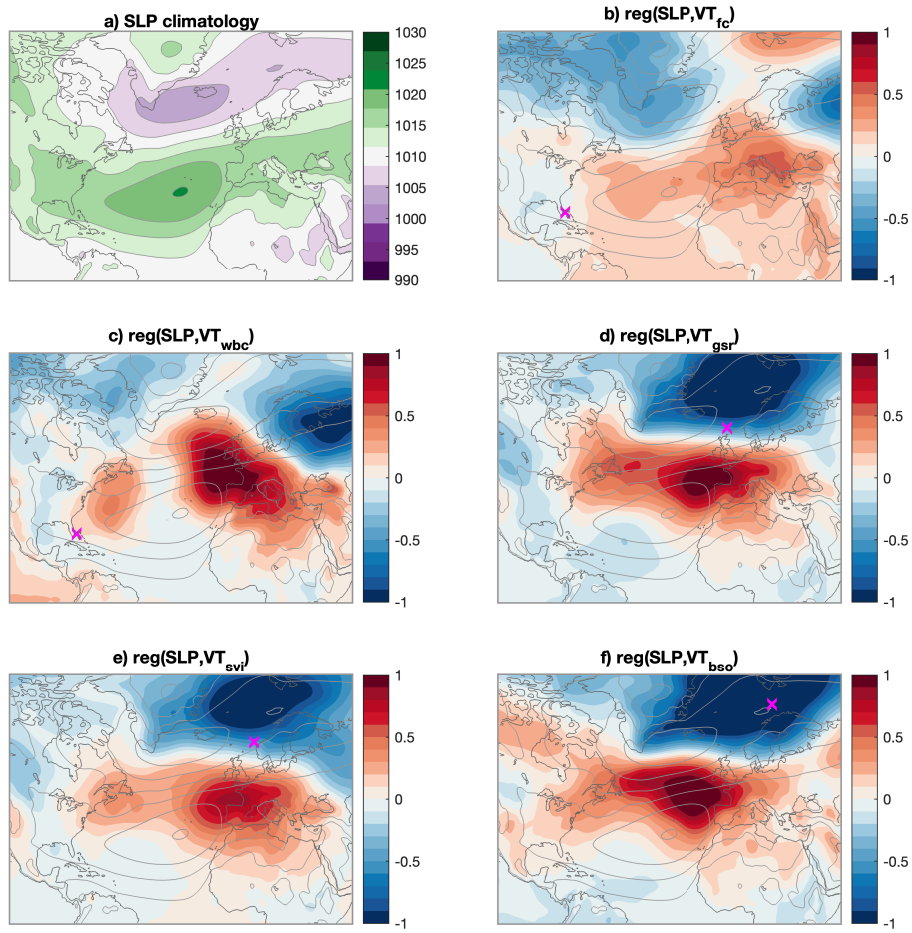


Figure S 7. ECCOv4-r4 transport variability and large-scale atmospheric circulation patterns for comparison with observations (Figure S8). (a) ECCOv4-r4 climatological sea level pressure (SLP; 1992-2017). Annual mean sea level pressure (hPa) regressed onto annual mean volume transport (VT; S_v) time series in ECCOv4-r4; (b) Florida Current (1992-2017), (c) Western Boundary Current at 26.5°N (wbc; 2005-2017), (d) Greenland-Scotland Ridge (gsr; 1995-2015), (e) NwASC at Svinøy (svi; 1996-2017), and (f) Barents Sea Opening inflow (bso; 1998-2016). Unit is hPa per standard deviation of volume transport. The volume transport time series has been normalized ($\frac{X - \mu_x}{\sigma_x}$) for comparable magnitudes between the panels. Gray contour lines show the climatological annual mean SLP pattern (contour interval: every 3 hPa from 1007 to 1019 hPa). The magenta cross marks the approximate location for the volume transport time series.

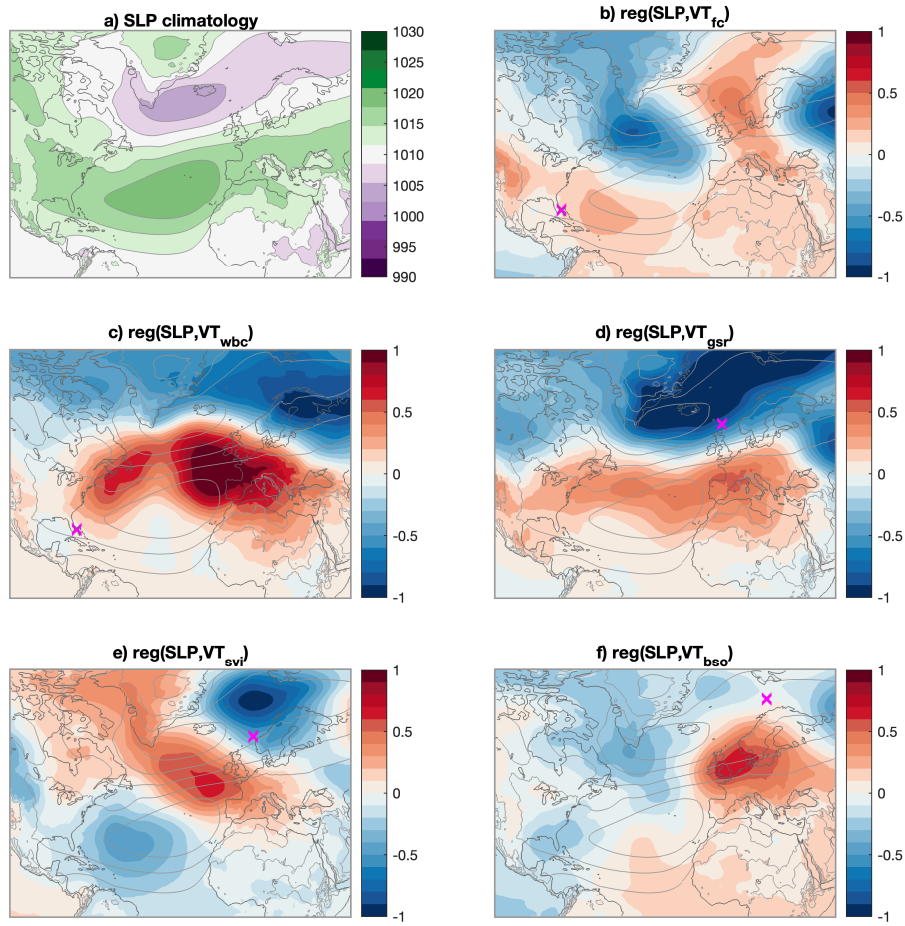


Figure S 8. Observed transport variability and large-scale atmospheric circulation patterns for comparison with ECCOV4-r4 (Figure S7). (a) ERA5 climatological sea level pressure (SLP; 1992-2017). ERA5 annual mean sea level pressure (hPa) regressed onto annual mean volume transport (VT; Sv) time series from observations; (b) Florida Current (1992-2017), (c) Western Boundary Current at 26.5°N (wbc; 2005-2017), (d) Greenland-Scotland Ridge (gsr; 1995-2015), (e) NwASC at Svinøy (svi; 1996-2017), and (f) Barents Sea Opening inflow (bso; 1998-2016). Unit is hPa per standard deviation of volume transport. The volume transport time series has been normalized ($\frac{X-\mu_x}{\sigma_x}$) for comparable magnitudes between the panels. Gray contour lines show the climatological annual mean SLP pattern (contour interval: every 3 hPa from 1007 to 1019 hPa). The magenta cross marks the approximate location for the volume transport time series.



Figure S 9. NAO and EAP indexes (as defined in Figure S1) accumulated over the 10 years prior.